2021 43rd Annual International Conference of the
IEEE Engineering in Medicine & Biology Society (EMBC)
Oct 31 - Nov 4, 2021. Virtual Conference

Bayesian Regularized Strain Imaging for Assessment of Murine Cardiac Function *In vivo*

Rashid Al Mukaddim, Ashley M. Weichmann, Rachel Taylor, Timothy A. Hacker, Thomas Pier, Melissa Graham, Carol C. Mitchell and Tomy Varghese

***Abstract*— A cardiac strain imaging framework with adaptive Bayesian regularization (ABR) is proposed for *in vivo* assessment of murine cardiac function. The framework uses ultrasound (US) radio-frequency data collected with a high frequency (f_c = 30MHz) imaging system and a multi-level block matching algorithm with ABR to derive inter-frame cardiac displacements. Lagrangian cardiac strain (radial, e_r and longitudinal, e_l) tensors were derived by segmenting the myocardial wall starting at the ECG R-wave and accumulating interframe deformations over a cardiac cycle. *In vivo* feasibility was investigated through a longitudinal study with two mice (one ischemia-perfusion (IR) injury and one sham) imaged at five sessions (pre-surgery (BL) and 1,2,7 and 14 days post-surgery). End-systole (ES) strain images and segmental strain curves were derived for quantitative evaluation. Both mice showed periodic variation of e_r and e_l strain at BL with segmental synchroneity. Infarcted regions of IR mouse at Day 14 were associated with reduced or sign reversed ES e_r and e_l values while the sham mouse had similar or higher strain than at BL. Infarcted regions identified *in vivo* were associated with increased collagen content confirmed with Masson's Trichrome stained *ex vivo* heart sections.**

***Clinical Relevance*— Higher quality cardiac strain images derived with RF data and Bayesian regularization can potentially improve the sensitivity and accuracy of non-invasive assessment of cardiovascular disease models.**

I. Introduction

Murine models of cardiovascular disease (e.g. myocardial infarction and ischemia-reperfusion injury) focus on providing mechanistic insight into disease progression and translation of pre-clinical therapies into clinics [1]. For accurate investigation of these models, non-invasive cardiovascular imaging plays a critical role [2]. In particular, ultrasound-based cardiac strain imaging has demonstrated higher sensitivity when compared to conventional echocardiography for assessing these models [3]. Cardiac strain imaging (CSI) is an ultrasound radio-frequency (RF) signal-based approach for estimation of myocardial tissue elasticity by utilizing the natural contraction and relaxation of the myocardium [4-11]. However, accurate strain estimation in murine models poses unique challenges due their small size and rapid heart rate [12]. Higher heart rate results in increased RF signal decorrelation and additional out-of-plane motion thus degrading CSI quality. To address these issues, we previously developed a multi-level block matching (BM) algorithm with Bayesian regularization for CSI [13-16]. Later, we developed an adaptive scheme which utilizes local RF data statistics to further optimize Bayesian regularization. In this paper, we report on a Lagrangian CSI framework incorporating Adaptive Bayesian Regularization [17] into a multi-level BM algorithm and investigate feasibility for longitudinal monitoring of cardiac remodeling in a murine model of ischemia-reperfusion injury *in vivo* with direct one-to-one histopathological validation.

This work is funded in part by UW-Madison Office of the Vice Chancellor for Research and Graduate Education from the Wisconsin Alumni Research Foundation and National Institutes of Health Grants S10 OD018505, 1R01 HL147866-01 and University of Wisconsin Carbone Cancer Center Support Grant P30 CA014520.

R. A. Mukaddim and T. Varghese are with the Department of Medical Physics, University of Wisconsin (UW) School of Medicine and Public Health (SMPH), Madison, and Department of Electrical and Computer Engineering, University of Wisconsin, Madison. A. M. Weichmann is with Small Animal Imaging and Radiotherapy Facility, UW Carbone Cancer Center. R. Taylor and T. J. Hacker are with Cardiovascular Physiology Core Facility, UW-Madison. T. Pier is with Experimental Animal Pathology Lab, UW-Madison. M. Graham is with Comparative Pathology Laboratory, Research Animal Resources and Compliance (RARC), UW-Madison. C. C. Mitchell is with the Department of Medicine/Division of Cardiovascular Medicine, UW-Madison.
(e-mail: mukaddim@wisc.edu).

II. Materials and Methods

A. In vivo Experimental Protocol

Two male BALB/CJ mice (one IR and one sham, acquired from The Jackson Laboratory, Bar Harbor, ME USA) were imaged pre-surgery (BL) and 1,2,7 and 14 days post-surgery. RF data collection was done using a MS 550D transducer (center frequency, f_c = 40 MHz) at 235 fps in the parasternal long axis view (Vevo 2100, Fujifilm Visualsonics). For the IR mouse, myocardial ischemia was first induced by ligation of the left anterior descending coronary artery (LAD) via thoracotomy and then blood flow was restored by releasing the tie after 45 minutes for reperfusion. Sham mouse underwent thoracotomy with no manipulation of the heart. After the 14 days post-surgery imaging session, the mice were euthanized, and hearts harvested for histopathological analysis. All *in vivo* experimental protocols were approved by the University of Wisconsin School of Medicine and Public Health Institutional Animal Care and Use Committee.

B. Locally Optimized Correlation Based Bayesian Adaptive Regularization (LOCBAR)

ECG and respiratory gating were applied offline to extract one cardiac cycle of RF data for cardiac strain imaging. To estimate interframe axial and lateral displacements, a three-level normalized cross-correlation (NCC) based block

matching (BM) algorithm [13, 18, 19] with locally optimized correlation based Bayesian adaptive regularization (LOCBAR) was utilized [17]. Bayesian regularization improves displacement estimation by enforcing spatial continuity in a local BM neighborhood through iterative application of Bayes theorem [20]. LOCBAR was developed to dynamically determine optimal iterations of Bayesian regularization per BM location by taking spatial and temporal strain heterogeneities expected *in vivo* into consideration. LOCBAR evaluates a local optimality criterion based on NCC signal-to-noise ratio and motion compensation between pre- and post-deformation RF frames to achieve dynamic regularization [17, 21]. For motion estimation, RF data were first interpolated laterally by a factor of 2 and then tracked with 2-D kernels with final dimensions of $[1\lambda, 11\ Alines]$ and [50%, 95%] overlap in the axial and lateral direction, respectively. Maximum allowed Bayesian iterations for LOCBAR was 10. For accurate sub-sample estimation, Sinc interpolation was utilized [22, 23]. Finally, 2-D median filtering was applied to remove any outliers.

C. *Lagrangian Cardiac Strain Estimation*

Myocardial walls were manually segmented at end-diastole (R-Wave of ECG) to generate a mesh of 24000 points covering the entire myocardium for accumulating interframe displacements over a cardiac cycle [24, 25]. The Lagrangian strain tensor, **E** was derived by estimating axial, lateral and shear strain components using a least squares strain estimator. Finally, radial (e_r) and longitudinal (e_l) strains were derived by applying coordinate transformation. Further details on Lagrangian strain estimation can be found here [24]. End-systole (ES) radial and longitudinal strain images were derived to qualitatively evaluate mouse cardiac function. Segmental radial and longitudinal strain curves over a cardiac cycle were also derived by dividing the myocardium into six segments (anterior base, anterior mid, anterior apex, posterior apex, posterior mid and posterior base denoted as segments 1 – 6) [26] and averaging strain values per segment. Finally, temporal progression of segmental ES strain values was compared between IR and sham mice.

D. *Histopathological Analysis*

Harvested myocardial tissue was sectioned in the long axis orientation and stained with Masson's trichome (MT) for quantification of fibrosis. To automatically classify regions of fibrosis, trainable Weka segmentation toolkit [27] was utilized to train machine learning model (https://imagej.net/Trainable_Weka_Segmentation). Finally, classified images from ImageJ [28] were loaded into MATLAB to quantify percentage of fibrosis in the infarcted and viable regions.

III. Results and Discussion

Figures 1 (a) – (b) show segmental radial and longitudinal strain curves respectively for the sham mouse at baseline derived with LOCBAR. Radial thickening [positive peak strain at Fig. 1 (a)] and longitudinal shortening [negative peak strain at Fig. 1 (b)] with synchroneity across myocardial segments was observed as expected at baseline thus indicating robust cardiac strain estimation with LOCBAR.

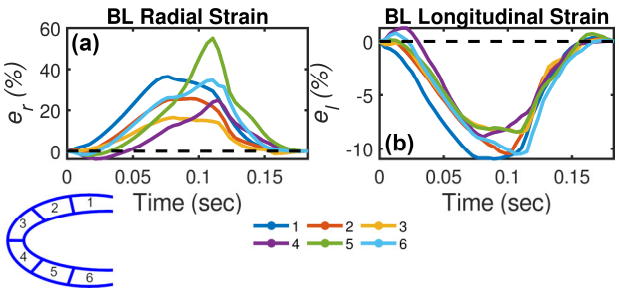

Fig. 1. Segmental (a) radial and (b) longitudinal strain curves for sham mouse at baseline.

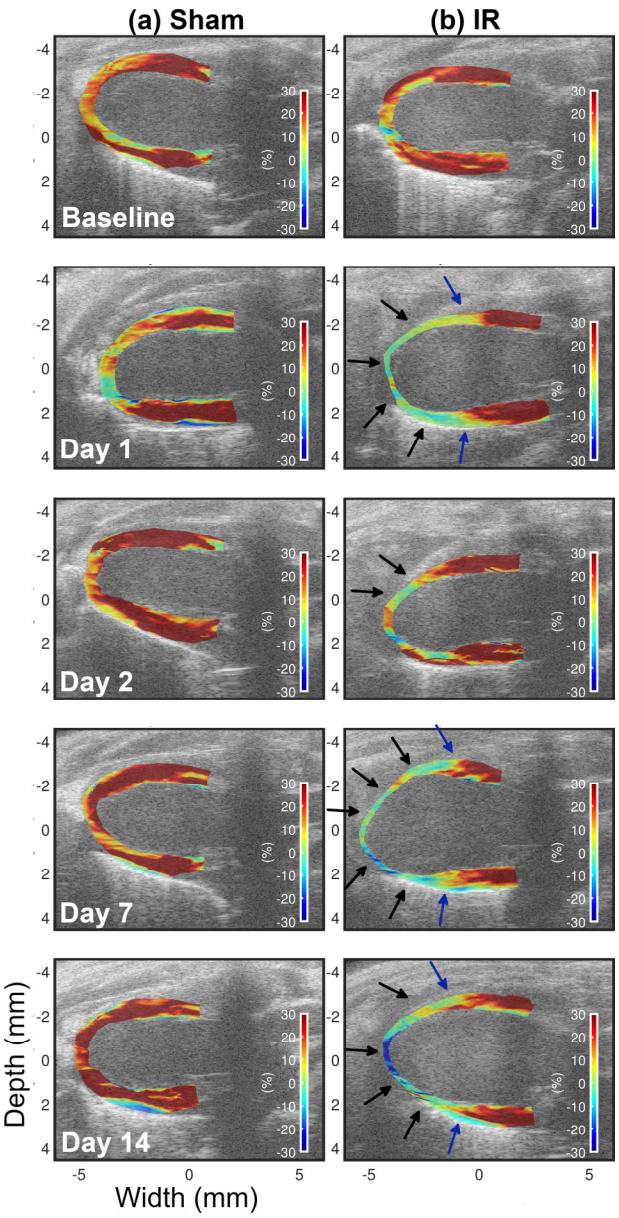

Fig. 2. ES accumulated radial strain images over time for (a) sham and (b) IR mice. Strain dynamic range is from -30% to +30%.

Figures 2 (a) – (b) show the progression of ES radial strain images over time for sham and IR mice, respectively. ES radial strain images for the sham mouse were predominately red except a portion of posterior mid segment at Day 14 indicating normal cardiac function radially [Fig. 2 (a)]. On the

other hand, post-surgery ES strain images for the IR mouse showed marked reduction or sign reversal of strain magnitudes (light green or blue) in the apical and mid segments when compared to baseline. Furthermore, infarct, border and viable regions can be clearly identified in the IR radial strain images having predominantly blue (black arrows), mixture of yellow + light blue + red (blue arrows), and red colors, respectively.

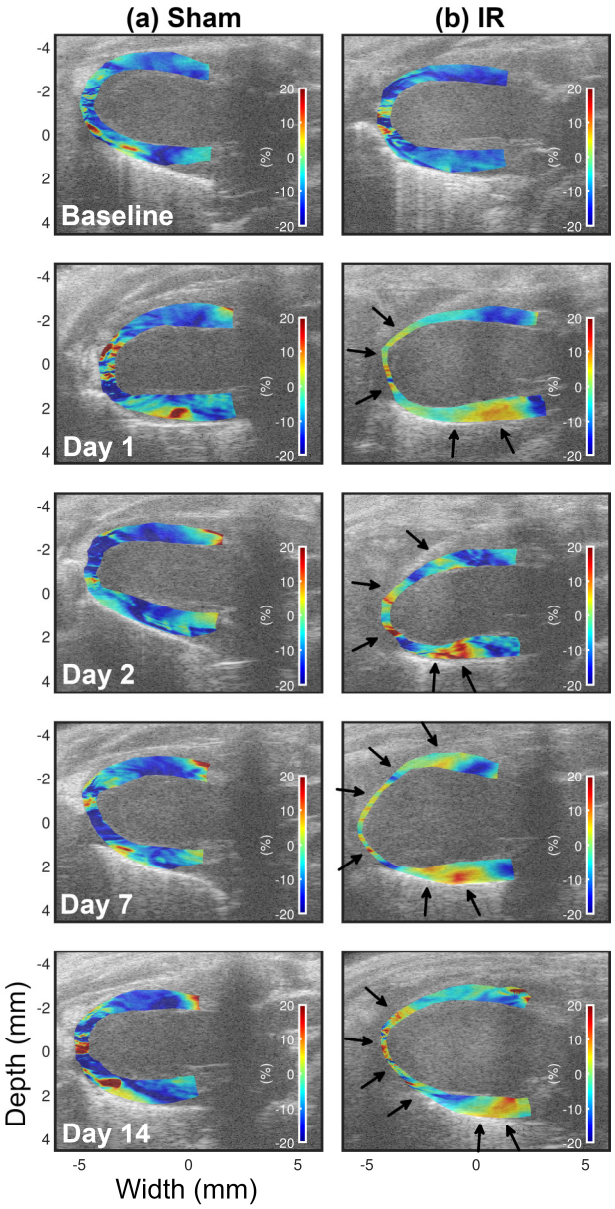

Fig. 3. ES accumulated longitudinal strain images over time for (a) sham and (b) IR mice. Strain dynamic range is from -20% to +20%.

Progression of ES longitudinal strain images over time for sham and IR mice are summarized in Figs. 3 (a) – (b) respectively. ES longitudinal strain images for the sham mouse were predominately blue except the posterior mid segment at Day 1, 7 and 14 (patch of positive strain values seen in red) indicating normal cardiac longitudinal shortening [Fig. 3 (a)]. For the IR mouse, post-surgery ES strain images showed marked reduction or sign reversal of strain magnitudes (red or light blue) with increased heterogeneity when compared to baseline indicating the impact of ischemia-reperfusion (observe black arrows).

Temporal progression of segmental ES radial and longitudinal strain values is summarized in Fig. 4. Fig. 4 (a) – (b) shows that the sham mouse had similar or higher strain (e_r and e_l) values when compared to baseline for all segments post-surgery except Day 1. For example, ES e_r values for anterior mid at BL = 25.61%, D1 = 15.74%, D2 = 52.11%, D7 = 38.01% and D14 = 37.73%. We observe some variability in day-to-day strain values attributed to reproducibility of probe positioning each day. For the IR case, clear separation in strain values between infarct and viable regions were observed. The infarcted regions showed steady decline in e_r strain values post-surgery (brown, green, gold and violet curves) while viable regions showed similar or higher strain values when compared to baseline (dark and light blue curves) [Fig. 4 (a)]. For example, ES e_r values for anterior mid (segment 2) at BL = 28.74%, D1 = 6.97%, D2 = 25.93%, D7 = 3.57% and D14 = 9.07%. Furthermore, a steady decline in e_l values for all segments were observed for the IR mouse post-surgery [Fig. 4 (b)]. For example, ES e_l values for anterior mid (segment 2) at BL = -11.66%, D1 = -5.79%, D2 = -6.28%, D7 = -1.72% and D14 = -5.14%.

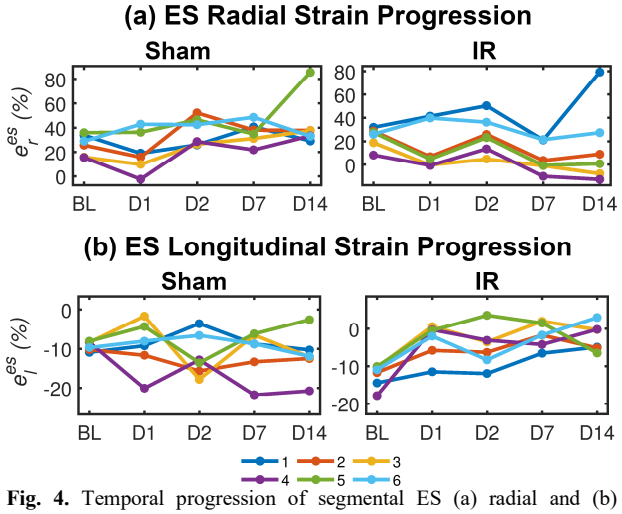

Fig. 4. Temporal progression of segmental ES (a) radial and (b) longitudinal strain values for sham and IR mouse. Segmentation is shown in Fig. 3.

Figures 5 (a) – (b) show the MT-stained heart sections for the sham and IR mouse, with segmented regions using Weka toolkit overlaid on these images. For the sham mouse, we observed uniform wall thickness with myocardial tissue appearing uniformly pink indicating absence of fibrosis. This corroborates with the *in vivo* strain images at D14 [Figs. 2 – 3], where uniform wall thickness was observed with high radial and longitudinal strain values. For IR, the presence of apical infarcts is clearly identified by observing wall thinning with infarcted regions appearing as light blue/gray and viable regions as pink (red and blue segmentations) thus corroborating our findings from *in vivo* cardiac strain imaging. Table I summarizes the relationship between global e_r and e_l strain values and collagen content expressed as percentage with respect to total area of the affected region. Table I shows that reduction in global strain values were associated with increased collagen content at Day 14. These

findings demonstrate that LOCBAR cardiac strain imaging was able to detect the areas with cardiac fibrosis *in vivo* non-invasively.

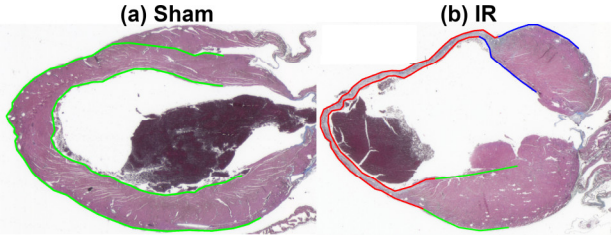

Fig. 5. Masson's trichrome stained (pink/light blue/gray colorization) heart sections for (a) sham and (b) IR mouse. Automatic segmentation using Weka toolkit is also overlaid on these images. Green = viable, red = infarct and blue = border region.

TABLE I
COMPARISON OF STRAIN AND HISTOPATHOLOGY AT DAY 14

	Global ES Strain (%)		Collagen Content (%)	
Mouse	e_r	e_l	**Infarct**	**Viable**
Sham	42.71	-11.68	×	1.76
IR	16.01	-2.32	88.77	2.13

IV. CONCLUSION

In this paper, we demonstrated Bayesian regularized strain imaging for assessment of murine cardiac function *in vivo*. The proposed framework differentiates cardiac remodeling associated with ischemia-reperfusion injury versus sham longitudinally over time. Furthermore, the strain variation observed *in vivo* corroborated our findings from *ex vivo* histopathological analysis. Future work will focus on validating the method in a larger cohort of mice and comparison against commercially available speckle tracking echocardiography solutions.

REFERENCES

[1] M. L. Lindsey, R. Bolli, J. M. Canty Jr, X.-J. Du, N. G. Frangogiannis, S. Frantz, *et al.*, "Guidelines for experimental models of myocardial ischemia and infarction," *American Journal of Physiology-Heart and Circulatory Physiology,* vol. 314, pp. H812-H838, 2018.

[2] C. K. Phoon and D. H. Turnbull, "Cardiovascular imaging in mice," *Current protocols in mouse biology,* vol. 6, pp. 15-38, 2016.

[3] M. Bauer, S. Cheng, M. Jain, S. Ngoy, C. Theodoropoulos, A. Trujillo, *et al.*, "Echocardiographic speckle-tracking based strain imaging for rapid cardiovascular phenotyping in mice," *Circulation research,* vol. 108, pp. 908-916, 2011.

[4] E. E. Konofagou, J. D'hooge, and J. Ophir, "Myocardial elastography—A feasibility study in vivo," *Ultrasound in medicine & biology,* vol. 28, pp. 475-482, 2002.

[5] T. Varghese, J. Zagzebski, P. Rahko, and C. Breburda, "Ultrasonic imaging of myocardial strain using cardiac elastography," *Ultrasonic imaging,* vol. 25, pp. 1-16, 2003.

[6] W.-N. Lee, "Myocardial elastography: a strain imaging technique for the reliable detection and localization of myocardial ischemia in vivo," COLUMBIA UNIVERSITY, 2010.

[7] J. Luo, K. Fujikura, S. Homma, and E. E. Konofagou, "Myocardial elastography at both high temporal and spatial resolution for the detection of infarcts," *Ultrasound in medicine & biology,* vol. 33, pp. 1206-1223, 2007.

[8] J. Luo and E. E. Konofagou, "High-frame rate, full-view myocardial elastography with automated contour tracking in murine left ventricles in vivo," *IEEE transactions on ultrasonics, ferroelectrics, and frequency control,* vol. 55, pp. 240-248, 2008.

[9] B. Chakraborty, Z. Liu, B. Heyde, J. Luo, and J. D'hooge, "2-D Myocardial Deformation Imaging Based on RF-Based Nonrigid Image Registration," *IEEE transactions on ultrasonics, ferroelectrics, and frequency control,* vol. 65, pp. 1037-1047, 2018.

[10] J. D'hooge, A. Heimdal, F. Jamal, T. Kukulski, B. Bijnens, F. Rademakers, *et al.*, "Regional strain and strain rate measurements by cardiac ultrasound: principles, implementation and limitations," *European Journal of Echocardiography,* vol. 1, pp. 154-170, 2000.

[11] S. Langeland, J. D'hooge, T. Claessens, P. Claus, P. Verdonck, P. Suetens, *et al.*, "RF-based two-dimensional cardiac strain estimation: a validation study in a tissue-mimicking phantom," *IEEE transactions on ultrasonics, ferroelectrics, and frequency control,* vol. 51, pp. 1537-1546, 2004.

[12] A. Bhan, A. Sirker, J. Zhang, A. Protti, N. Catibog, W. Driver, *et al.*, "High-frequency speckle tracking echocardiography in the assessment of left ventricular function and remodeling after murine myocardial infarction," *American Journal of Physiology-Heart and Circulatory Physiology,* vol. 306, pp. H1371-H1383, 2014.

[13] R. Al Mukaddim, N. H. Meshram, C. C. Mitchell, and T. Varghese, "Hierarchical Motion Estimation With Bayesian Regularization in Cardiac Elastography: Simulation and In Vivo Validation," *IEEE transactions on ultrasonics, ferroelectrics, and frequency control,* vol. 66, pp. 1708-1722, 2019.

[14] R. Al Mukaddim and T. Varghese, "Improving Ultrasound Lateral Strain Estimation Accuracy using Log Compression of Regularized Correlation Function," *2020 42nd Annual International Conference of the IEEE Engineering in Medicine and Biology Society (EMBC). IEEE,* 2020.

[15] R. Al Mukaddim, K. Samimi, A. Rodgers, T. A. Hacker, and T. Varghese, "Comparison of cardiac displacements in a murine model of myocardial ischemia using Cardiac Elastography and speckle tracking echocardiography," in *2017 IEEE International Ultrasonics Symposium (IUS)*, 2017, pp. 1-4.

[16] R. Al Mukaddim and T. Varghese, "Cardiac Strain Imaging with Dynamically Skipped Frames: A Simulation Study," in *2020 IEEE International Ultrasonics Symposium (IUS)*, 2020, pp. 1-4.

[17] R. Al Mukaddim, N. H. Meshram, and T. Varghese, "Locally optimized correlation-guided Bayesian adaptive regularization for ultrasound strain imaging," *Physics in Medicine & Biology,* vol. 65, p. 065008, 2020.

[18] H. Shi and T. Varghese, "Two-dimensional multi-level strain estimation for discontinuous tissue," *Physics in medicine and biology,* vol. 52, p. 389, 2007.

[19] H. Chen, H. Shi, and T. Varghese, "Improvement of elastographic displacement estimation using a two-step cross-correlation method," *Ultrasound in medicine & biology,* vol. 33, pp. 48-56, 2007.

[20] M. McCormick, N. Rubert, and T. Varghese, "Bayesian regularization applied to ultrasound strain imaging," *IEEE Transactions on Biomedical Engineering,* vol. 58, pp. 1612-1620, 2011.

[21] C. C. Mitchell, R. Al Mukaddim, A. M. Weichmann, K. W. Eliceiri, M. E. Graham, and T. Varghese, "Carotid Strain Imaging with a Locally Optimized Adaptive Bayesian Regularized Motion Tracking Algorithm," in *2020 IEEE International Ultrasonics Symposium (IUS)*, 2020, pp. 1-4.

[22] N. H. Meshram and T. Varghese, "GPU accelerated multilevel Lagrangian carotid strain imaging," *IEEE transactions on ultrasonics, ferroelectrics, and frequency control,* vol. 65, pp. 1370-1379, 2018.

[23] M. M. McCormick and T. Varghese, "An approach to unbiased subsample interpolation for motion tracking," *Ultrasonic imaging,* vol. 35, pp. 76-89, 2013.

[24] R. Al Mukaddim, N. H. Meshram, C. C. Mitchell, and T. Varghese, "Hierarchical Motion Estimation with Bayesian Regularization in Cardiac Elastography: Simulation and in-vivo Validation," *IEEE transactions on ultrasonics, ferroelectrics, and frequency control,* 2019.

[25] C. Ma and T. Varghese, "Lagrangian displacement tracking using a polar grid between endocardial and epicardial contours for cardiac strain imaging," *Medical physics,* vol. 39, pp. 1779-1792, 2012.

[26] M. L. Lindsey, Z. Kassiri, J. A. Virag, L. E. de Castro Brás, and M. Scherrer-Crosbie, "Guidelines for measuring cardiac physiology in mice," *American Journal of Physiology-Heart and Circulatory Physiology,* vol. 314, pp. H733-H752, 2018.

[27] I. Arganda-Carreras, V. Kaynig, C. Rueden, K. W. Eliceiri, J. Schindelin, A. Cardona, *et al.*, "Trainable Weka Segmentation: a machine learning tool for microscopy pixel classification," *Bioinformatics,* vol. 33, pp. 2424-2426, 2017.

[28] J. Schindelin, I. Arganda-Carreras, E. Frise, V. Kaynig, M. Longair, T. Pietzsch, *et al.*, "Fiji: an open-source platform for biological-image analysis," *Nature methods,* vol. 9, pp. 676-682, 2012.